Chapter 2

Interaction of Tropical Cyclones with a Dipole Vortex

Ismael Perez-Garcia, Alejandro Aguilar-Sierra and Jaime Hernández

Additional information is available at the end of the chapter

http://dx.doi.org/10.5772/65953

Abstract

The purpose of this chapter is to discuss certain disturbances around the pole of a Venus–type planet that result as a response to barotropic instability processes in a zonal flow. We discuss a linear instability of normal modes in a zonal flow through the barotropic vorticity equations (BVEs). By using a simple idealization of a zonal flow, the instability is employed on measurements of the upper atmosphere of Venus. In 1998, the tropical cyclone Mitch gave way to the observational study of a dipole vortex. This dipole vortex might have helped to intensify the cyclone and moved it towards the SW. In order to examine this process of interaction, the nonlinear BVE was integrated in time applied to the 800–200 hPa average layer in the previous moment when it moved towards the SW. The 2-day integrations carried out with the model showed that the geometric structure of the solution can be calculated to a good approximation. The solution HLC moves very fast westwards as observed. On October 27, the HLA headed north-eastward and then became quasi-stationary. It was also observed that HLA and HLC as a coupled system rotates in the clockwise direction.

Keywords: polar vortices Venus, barotropic vorticity equation, normal mode instability, tropical cyclone, American monsoon system.

1. Introduction

The air at the equatorial regions rises when heated by the sun and as it does, it cools down and sinks. Rising air creates low pressure, sinking air creates high pressure. High altitude winds move towards the poles and surface winds move towards the equator, creating a simple convective motion known as the Hadley cells. These Hadley cells are the atmospheric circulation system driven by solar heated ground. On Earth, the Coriolis effect breaks each circulation

cell into several separate cells, which are easily visible from space. Global circulation or local weather systems moves from West to East at mid–latitudes in the Northern Hemisphere (NH). Two main factors that cause these patterns are atmospheric heating and planetary rotation.

Vortices are structures observed in planets with atmospheres. Earth, Mars, Venus, Jupiter and Saturn. On Earth, these atmospheric vortices are called cyclones and anticyclones. A cyclone or "Low" is a storm or a system of winds that rotates around a centre of low atmospheric pressure. An anticyclone or "High" is a system of winds that rotates around a centre of high atmospheric pressure.

Winds in a cyclone blow counterclockwise in the NH while they move clockwise in the Southern Hemisphere (SH). Winds in an anticyclone blow in the opposite direction. Cyclones that form over tropical regions are called tropical cyclones. The semi-permanent and transient cyclones or anticyclones are associated with weather systems. Polar vortex, Bermuda High, the Siberian High and the Aleutian Low are examples of semi-permanent systems. The subtropical high pressure belts that exist in the atmosphere overlaps with the descending legs of the Hadley cells. These semi-permanent subtropical centres of high pressure develop as direct responses to solar heating produced by the differential heating of continents and oceans. The role of the cyclones and anticyclones in the general circulation of the atmosphere is to exchange heat and moisture between the equator and the poles.

The polar vortex, also called "Circumpolar vortex", is an upper level low-pressure zone, with a prevailing wind pattern that circulates in the Arctic, flowing from west to east lying near the Earth's pole, that is usually kept in place by the jet stream that divides cold air from warm air. The jet stream is a relatively narrow band of strong winds in the upper levels of the atmosphere that blow from West to East; however, it often shifts to the North or South. The strongest occurrence of jet stream takes place during both the Northern and Southern Hemisphere winters. The 50° –60° N/S region is where the polar jet is located with the subtropical jet near 30° N. The interface between the cold dry air mass from the pole and the warm moist air mass from the south, defines the location of the polar front, extending from the surface up to the troposphere. An upper-level front on Earth is usually associated with the mid-latitude jet [1], while the cold collar on Venus is a ring of cooler air that surrounds the polar vortex and which denotes a darker area between 60° and 80° [2].

The Earth and Venus are about the same size. Venus has a radius of $a_v = 6051.8$km and the Earth has a mean radius $a = 6371$ km. Venus moves around the Sun, completing one orbit in every 224 earth days. Most of the planets and the sun in our solar system rotate in the counterclockwise direction when viewed from above their North Poles. Venus, however, rotates in the opposite direction. Venus spins extremely slowly, completing one rotation every 243 earth days, so on Venus the Coriolis effect is very weak. It is also weak in Earth's tropics. A day in Venus is longer than its year. Venus's retrograde turn means that the planet's North Pole actually lies below the ecliptic plane.

The atmosphere on Venus is extremely dense, the temperature increases downwards from 100 to 40 km except in an inversion layer about 60–70km. The range of 1–360mbar have altitudes of 55–85 km, with surface pressures of 90 mbar and clouds beginning at 43 km [3]. In 1974, a

http://dx.doi.org/10.5772/65953

hemispheric vortex centred at the South Pole of Venus was observed at the time of Mariner 10. In 1979, images of Venus from Pioneer showed a similar vortex at North Pole. The winds were stronger at the equator, and slowed down towards the poles, creating a visible "V" shape on images of the cloud layers. In fact, the Venus clouds upper-deck rotates around the planet in just 4–5 days, which is in a much faster pace than in the underlying surface [4]. This is called super-rotation, because it is in the same direction as the rotation of the planet, but much stronger. The super-rotation is not that of an actual rigid body. Two essential questions remain to be answered: what are these eddies at the polar region? Where do they come from? They come from the processes of barotropic instability [5]. In Section 2, the fact that certain disturbances around the Venus pole arise as a response to barotropic instability processes of a zonal flow is demonstrated.

On Earth, tropical cyclones originate over tropical or subtropical regions in the Indian Ocean, western North Pacific and South Pacific Ocean, forming between 5° and 30° N and typically move westwards, north and north-westwards. When tropical cyclones reach subtropical latitudes, they often move north-eastwards. Also, the coasts of Mexico and Central America are influenced by the presence of the northern Atlantic and north-eastern Pacific tropical cyclones. A question remains to be answered on the movement of tropical cyclones: what pushes them south-westward. In particularly, tropical cyclone Mitch moved south-westward by October 26–30, [6]. The overall motion of Mitch was slow, less than 5mph, this resulted in a tremendous amount of rainfall, primarily over Central America, which killed thousands of people. Section 3 of this present chapter, provides an observational study of a dipole vortex associated with the tropical cyclone Mitch, and the barotropic vorticity equations (BVEs) used to study the movement toward Southwest. The dipole vortex is an interesting feature that occurs during the intersection of the local summer months (September–November), formed in coupled monsoon systems: the late North American monsoon system (NAMS) and early South American monsoon system (SAMS).

2. Polar vortices in planetary atmosphere

A polar vortex, also known as the "Circumpolar Whirl", is a large-scale circulation in the middle and upper troposphere, generally centred in the Polar Regions. These polar vortices form when heated air from equatorial latitudes rises, and then spirals towards the poles. In fact, the upper deck of clouds on Venus rotates around the planet much faster than the underlying surface. This is also called super-rotation, because the rotation is in the same direction as the rotation of the planet, but faster [4].

At the cloud top altitude of 67–72km, the main properties of the mean zonal velocity profile are well known. Hueso and Sanchez-Lavega [3] presented an update on the average zonal and meridional mean profile wind of the upper cloud at 66–73km for Venus SH from −90° to near −5° as observed with VIRTIS-M UV day-side data. Comparing with previous results by Sanchez-Lavega [7] and Moissl [8], they present the same general behaviour at all altitudes. Moissl [8] showed that a profile zonal wind from −85° to 20° with a zonal wind speed of

85° −90m/s almost constant with latitude is observed at low latitudes. The latitude zonal wind profile shows a gradually increase reaching 100m/s near 45° S, indicating the presence of a weak midlatitude jet. South of this latitude the wind speed decreases to zero towards the poles.

We assume that there is a similar circulation in the Northern Hemisphere in Venus, as observed in the "V" shaped clouds that move westwards. Therefore, we may be reconstructing a simple idealization of a symmetric zonal flow around Venus' equator based on the measurements taken from the upper atmosphere of Venus broadly consistent with the work of Refs. [3, 7, 8, 9]. This latitude profiles of symmetric zonal wind at the upper cloud layer at 66–73km is shown in **Figure 1**.

In latitudes between −50° and 50°, strong winds of up to 100 m/s with –10 m/s oscillations were observed. In latitudes between −4° and 4° strong winds of up to −108 m/s were observed, indicating the presence of a weak jet near the equator. Zonal winds closer to the poles gradually slowdown at latitude of about 48° on Venus. In both the Northern and Southern Hemispheres a small jet stream was found along with a meridional shear of $\frac{\partial u}{\partial y} = -0.027 \mathrm{ms}^{-1}\mathrm{km}^{-1}$ [3].

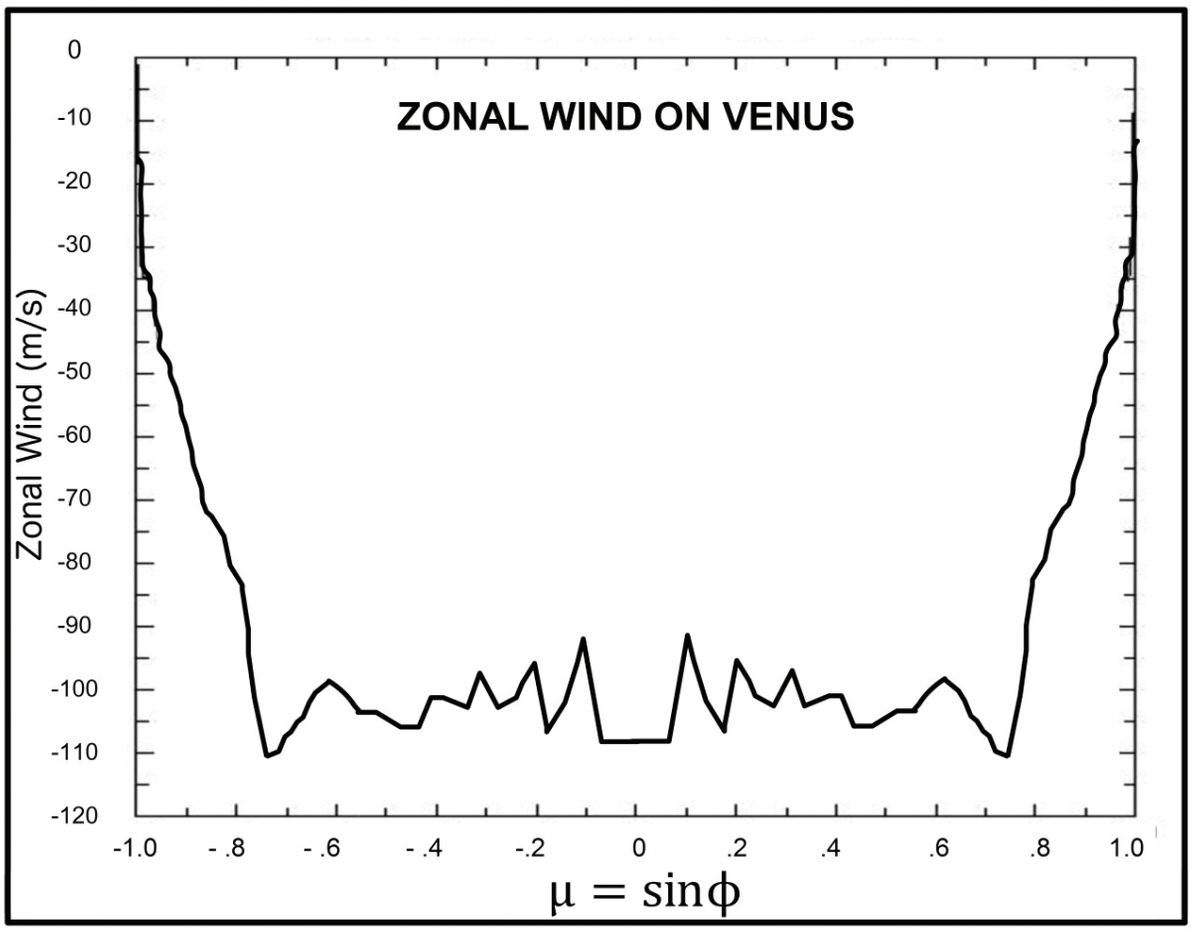

Figure 1. Zonal wind profiles idealized at the upper cloud layer of Venus taken and adapted from Ref. [3]. The horizontal axis is $\mu = \sin\phi$.

Venus' atmosphere can be divided into two broad layers. The first layer rotates in 4 Earth days and the second one is underneath. Let the height of Venusian atmosphere be H_v, we may consider that the Venusian atmosphere resides between two concentric spheres with different radii a_v and $a_{v_t} = a_v + H_v$. Assuming that the mean level of this spherical shell rotated around the planet in just 4 Earth days or at an angular velocity $\Omega_{v_a} = -2.893 \times 10^{-6} s^{-1}$, it would be much faster than the underlying surface or Venus angular velocity $\Omega_v = -3 \times 10^{-7}$ s^{-1}.

Widely used to understand many features of the large scale dynamics of the barotropic Earth atmosphere, we might consider the vertical component of the barotropic vorticity equation (BVE) for an ideal fluid non-divergent on a unit sphere S, which can be written in the non-dimensional form as follows [10]:

$$\frac{\partial \Delta \Psi}{\partial t} + J(\Psi, \Delta \Psi + 2\mu) = 0 \tag{1}$$

where $\Psi(\lambda, \mu)$ denotes the stream function. The spherical coordinates are longitude λ, latitude ϕ or $\mu = \sin\phi, -\pi \leq \lambda \leq \pi, -\frac{\pi}{2} \leq \phi \leq \frac{\pi}{2}$. Δ is the Laplace operator on a sphere and $J(\Psi, \eta)$ is the Jacobian operator. The equation is non-dimensionalized with the Earth radius a as the length scale and the inverse of the Earth angular velocity $7.292 \times 10^{-5} s^{-1}$ as the timescale. The relative vorticity is $\xi = \Delta \Psi$ and the absolute vorticity is $\eta = \xi + 2\mu$. On Venus, the Coriolis parameter would be neglected, since it is two orders of magnitude lower than the Earth's one. The relative vorticity expressed in terms of wind vector (u, v):

$$\xi(\lambda, \mu) = \frac{1}{\sqrt{1-\mu^2}} \frac{\partial v}{\partial \lambda} - \sqrt{1-\mu^2} \frac{\partial u}{\partial \mu} + \frac{\mu u}{\sqrt{1-\mu^2}} \tag{2}$$

Where

$$u = -\sqrt{1-\mu^2} \frac{\partial \Psi}{\partial \mu}, \; v = \frac{1}{\sqrt{1-\mu^2}} \frac{\partial \Psi}{\partial \lambda} \tag{3}$$

are the velocity components that relates to the stream function.

Eq. (1) captures many features of the large scale dynamics of the barotropic Earth's atmosphere, providing better understanding of the low–frequency variability, teleconnection patterns and the synoptic blocking events [11–15]. A mechanism that generates low-frequency variability is the instability of non-zonal basic flow as proposed by Simmons et al. [11]. The four classes of BVE (for ideal flow) solutions known by now are the simple zonal flows $\tilde{\Psi}(\mu)$ and more complicated flows called Rossby–Haurwitz (RH) waves, Wu–Verkley waves [16] and modons [17–21].

The temperature and pressure on Earth are similar to those above 50 km on Venusian atmosphere. This implies that Earth's BVE can be applied to Venus middle atmosphere [2, 5]. The instability caused by the existence of a sufficiently large horizontal shear in the wind field of a basic flow is known as barotropic instability [22]. In continuation with the study of that polar

dipole vortex might result from the barotropic and baroclinic instabilities of the Venusian atmosphere [5, 23–25]. We were interested in exploring the instability of a zonal flow in super-rotation and the instability of zonal basic flow as shown in **Figure 1**.

In order to examine the resulting perturbation in the linear barotropic model, Skiba and Perez–Garcia [26] developed a numerical spectral method for normal mode stability study of ideal flows on a rotating sphere, which was tested on zonal flows [27].

The linearized equation for $\xi^{'}$ is:

$$\frac{\partial \xi^{'}}{\partial t} + J(\tilde{\Psi}, \xi^{'} + 2\mu) + J(\Delta^{-1}\xi^{'}, \tilde{\xi} + 2\mu) = 0, \tag{4}$$

Where $\xi^{'} = \Delta\psi^{'}$ is relative vorticity of the perturbation, the wide tilde mark represents basic flow, and primes refer to infinitesimal perturbation. In the form of a normal mode

$$\psi^{'}(\lambda, \mu, t) = \hat{\Psi}(\lambda, \mu)e^{\omega t}, \;\; \xi^{'}(\lambda, \mu, t) = \Delta\hat{\Psi}(\lambda, \mu)e^{\omega t} = G(\lambda, \mu)e^{\omega t}, \tag{5}$$

leads to the spectral problem

$$LG = \omega G \tag{6}$$

For the linearized operator $\mathrm{L}G = J(\tilde{G}, \Delta^{-1}G) – J(\tilde{\Psi}, G)$, $\omega = \omega_r + i\omega_i$, is the eigenvalue, G the eigenfunction and $\hat{\Psi}(\lambda, \mu) = \hat{\Psi}_r(\lambda, \mu) + i\hat{\Psi}_i(\lambda, \mu) = |\hat{\Psi}(\lambda, \mu)|e^{i\theta}$ is the amplitude. Here $\theta(\lambda, \mu) = \arg\,\theta(\lambda, \mu) = \arctan\left\{\frac{\hat{\Psi}_r(\lambda, \mu)}{\hat{\Psi}_i(\lambda, \mu)}\right\}$ is the initial phase of the mode. In the normal mode (linear) stability analysis, the basic state must be regarded as a steady state. A mode $\psi^{'}$ is unstable if $\omega_r > 0$, decaying if $\omega_r < 0$, neutral if $\omega_r = 0$, and stationary if $\omega_i = 0$.

A zonal basic flow with horizontal shear can be constructed analytically by $\tilde{\Psi}(\mu) = w\,P_n(\mu)$ in which $P_n(\mu)$ is a Legendre Polynomial (LP), with $\mu = \sin\phi$, and w, an arbitrary constant. The simplest super-rotation zonal flow is analytically constructed so that the equatorial easterly jet streams (the mean zonal wind in the equatorial latitude is −105 m/s decreasing to zero at the pole) are preserved with a weak easterly wind around poles: $\tilde{\Psi}(\mu) = -wP_1(\mu) = -w\mu (w = -0.226$ is the rotation velocity). We used the Rayleigh-Kuo necessary condition for the instability [28, 29]: Let $\tilde{\Psi}(\mu)$ be a zonal flow on the sphere, then a normal mode may be unstable only if the derivative $\frac{\partial\tilde{\eta}}{\partial\mu}$ of the absolute vorticity $\tilde{\eta} = \tilde{\Psi}(\mu) + 2\mu$ changes its sign at least in one point of the interval $(-1, +1)$. Since in the mean level of Venus' atmosphere the absolute vorticity $\tilde{\eta} = \tilde{\Psi}(\mu) + 2r\mu$, where $r = -3.96\times10^{-2}$, then in our case, $\frac{\partial\tilde{\eta}}{\partial\mu} = 2(w + r)$ is a constant and hence there is no unstable normal mode, this is neutral. However for the zonal flow $\tilde{\Psi}(\mu) = wP_n(\mu)$, $\frac{\partial\tilde{\eta}}{\partial\mu} = 2r - w\chi_n\frac{\partial P_n}{\partial\mu}$ where $\chi_n = n(n + 1)$, then there is a critical amplitude w for developing the instability, due to the sphere rotation [26, 27].

Rossby-Haurwitz wave has proved to be very useful in interpreting the large-scale wave structures in the Earth atmospheric circulation of middle latitudes. Not only should the zonal wind profile be consistent with Venusian climatology (**Figure 1**), but attention must also be given to the absolute vorticity of the zonal flow in the equatorial region. The effect of the mean flow, given by a linear combination Legendre polynomials and a Rossby-Haurwitz wave, was provied by Refs. [15, 27]. The zonal basic flow, demonstrated in **Figure 2**, can be approximated by the following,

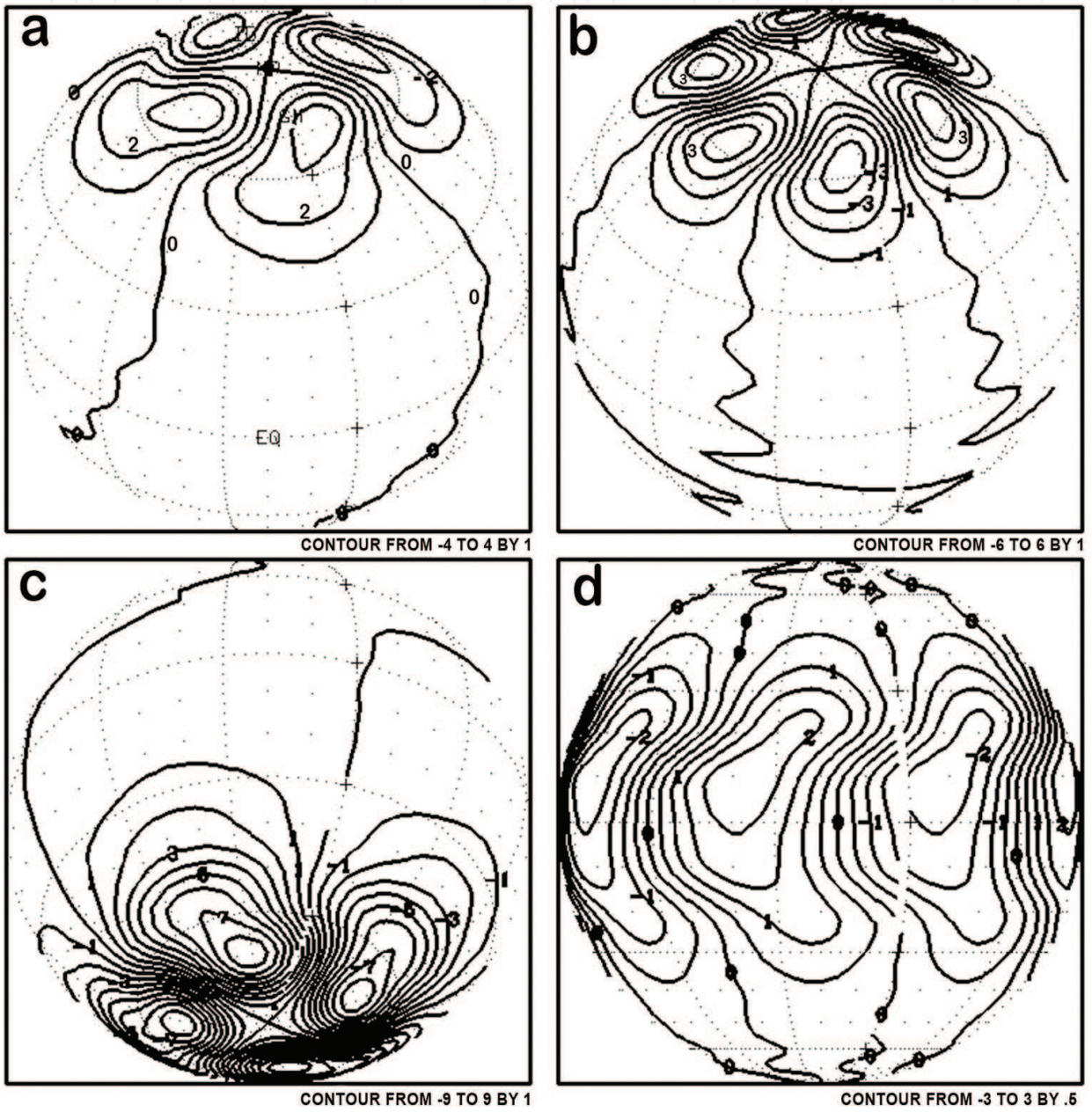

Figure 2. Isolines of the amplitudes $\hat{\Psi}_r(\lambda, \mu)$ of four most unstable modes corresponding to: $\omega_r = 86.08$ (a), $\omega_r = 64.31$ (b), $\omega_r = 67.23$ (*c*) and $\omega_r = 47.61$ (d).

$$\tilde{\Psi}(\mu) = \sum_{j=0}^{5} w_{2j+1} P_{2j+1}^{0}(\mu) + \sum_{j=1}^{2} w_{2j} P_{2j}^{0}(\mu), \tag{7}$$

where $P_n^m(\mu)$ is the associated Legendre function of degree n and zonal wave number m, and w' are constants and w_5 is very small. Then,

$$\frac{\partial \tilde{\eta}}{\partial \mu} = 2r - \sum_{j=0}^{5} \chi_{2j+1} w_{2j+1} \frac{\partial P_{2j+1}^{0}}{\partial \mu} - \sum_{j=1}^{2} \chi_{2j} w_{2j} \frac{\partial P_{2j}^{0}}{\partial \mu} \tag{8}$$

changes its sign at least in one point of the interval $(-1, +1)$, and thus Eq. (7) may have unstable normal modes.

Observational evidence indicates that the zonal flow pattern on the Earth can be approximately represented by a linear combination of seven Legendre polynomials of odd parity [15, 30]. The zonal flow has the maximum westerly of 33m/s at 35° North and South, and an easterly wind of 5m/s at the equator. This zonal wind field resembles the upper troposphere during the northern winter. The stability analysis showed that unstable perturbations are observed in the neighbourhood of subtropical jets, and the dominant zonal wave number of the modes are m = 7 and m = 5 (see **Figure 3** of [15]).

However, Skiba [31] showed that for a zonal flow PL and a RH wave, the amplitude $\hat{\Psi}$, of each unstable or decaying mode must satisfy the condition,

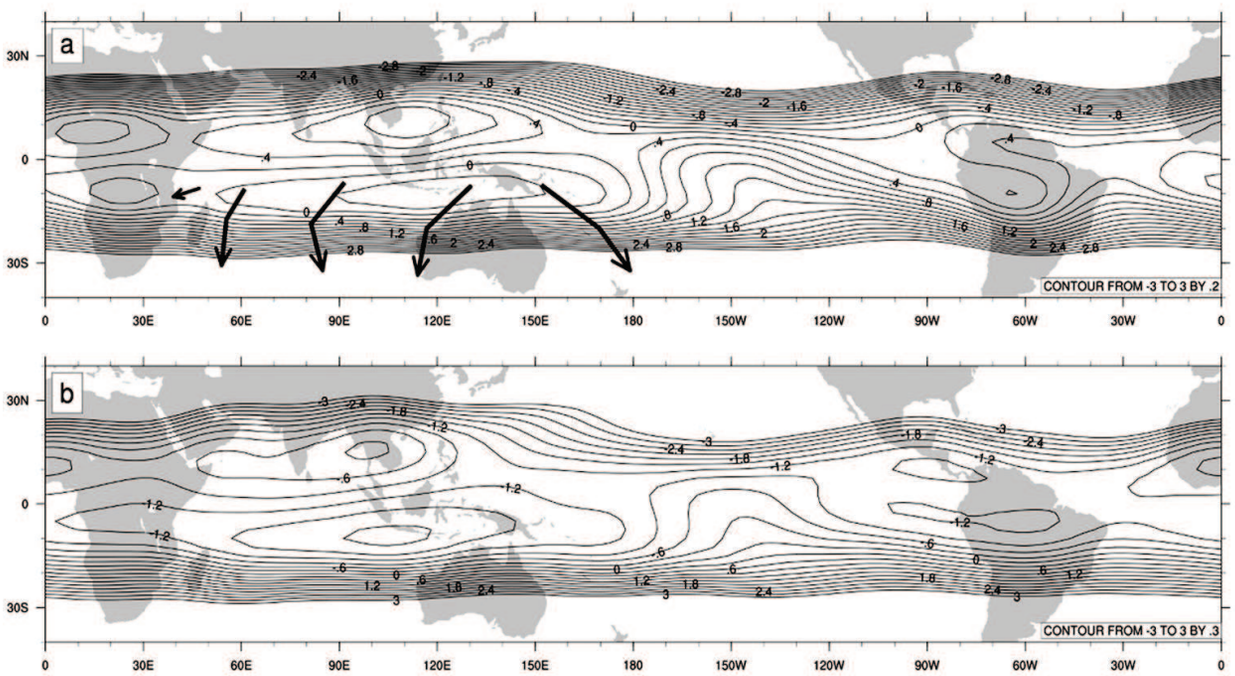

Figure 3. Isolines of the monthly stream function multiplied by 10^7 for April (a) and May (b) mean 200-250 mbar respectively. Tropical cyclone tracks in (a) are adapted from Ref. [36].

Modes	ω_r	ω_i	$\chi_{\hat{\Psi}}$	τ_e	T
1	86.03	215.53	86.26	1.84×10^{-3},	4.63×10^{-3},
2	64.28	−309.52	89.39	2.47×10^{-3},	3.23×10^{-3},
3	57.16	236.45	76.94	2.78×10^{-3},	4.22×10^{-3},
4	47.63	66.01	56.55	3.34×10^{-3},	1.51×10^{-2},

Table 1. The most unstable mode of the Venus' polar zonal flow described by **Figure 2**.

$$\chi_{\hat{\Psi}} = \frac{E(\hat{\Psi})}{k(\hat{\Psi})} \tag{9}$$

where $\chi_{\hat{\Psi}}$ is the square of Fjörtoft's [32] average spectral number of the mode amplitude $\hat{\Psi}$, and $\mathrm{K}(\hat{\Psi}) = \frac{1}{2}\,\|\nabla\hat{\Psi}\|^2 = \frac{1}{2}\sum_{n=1}^{\infty}\chi_n\sum_{m=-n}^{n}\left|\hat{\Psi}_n^m\right|^2$ and $\mathrm{E}(\hat{\Psi}) = \frac{1}{2}\,\|\Delta\hat{\Psi}\|^2 = \frac{1}{2}\sum_{n=1}^{\infty}\chi_n^2\sum_{m=-n}^{n}\left|\hat{\Psi}_n^m\right|^2$ are the total kinetic energy, and entrophy of $\hat{\Psi}$, and $\hat{\Psi}_n^m$ is the Fourier coefficient.

In this part of our chapter we shall study the normal mode numerical stability, in the case of zonal flow in **Figure 1**, then Eq. (6) is solved by representing all variables as series of spherical harmonics, by employing triangular truncation T21 and by taking the Coriolis parameter as $2r\mu$. The main parameters of the first four most unstable modes, $\omega = \omega_r + i\omega_i$, spectral number $\chi_{\hat{\Psi}}$ of the mode amplitude, e-folding time $\tau_e = \frac{1}{2\pi|\omega_r|}$ and period $T = \frac{1}{|\omega_i|}$ of the mode are given in **Table 1**.

As shown in **Figure 2**, for the first two most unstable modes, disturbances are located at the northern side of the largest jet stream of the North Hemisphere and for the third most unstable mode the disturbances are generated at the southern side of the largest jet stream in the South Hemisphere. From Ref. [26] we get the equation that describes the evolution of the total kinetic energy $K(\psi')$ of an infinitesimal perturbation ψ' to a zonal flow $\tilde{\Psi}(\mu)$ on sphere S,

$$\frac{dK(\psi')}{dt} = -\int\sqrt{1-u^2}(u'v')\cdot\frac{\partial\tilde{u}}{\partial\mu}\,ds - \int\frac{\mu}{\sqrt{1-\mu^2}}(u'v')\cdot\tilde{u}\,ds \tag{10}$$

The sign of $\frac{dK(\psi')}{dt}$ depends on the signs of the products $(u'v')\cdot\tilde{u}$ and $(u'v')\cdot\frac{\partial\overline{u}}{\partial\mu}$ in various regions of the sphere. In regions of generation of the energy of perturbations, the inclination of main axes of localized perturbations in the stream function field must be opposite to the inclination of zonal velocity profile, that is, in the regions where product $(u'v')\cdot\frac{\partial\overline{u}}{\partial\mu}$ is positive [11]. Whereas the first integral dominates principally at the sides of the jets located in the tropics and mid-latitudes, the second integral can be significant in the central parts of strong jets, especially when such jets are located in the polar regions, where $\frac{\mu}{\sqrt{1-\mu^2}}$ is large [26, 27]).

Figure 2(d) shows the four modes most unstable with the V shapes, along the equatorial region. Data from the Vertis on Venus Express [33], also near the equator, show that similar

"V" structure of cloud layers were observed, as shown in this chapter, which could be associated with the barotropic instability processes. Further experiments were performed with different values for $r = \frac{\Omega_v}{\Omega} = 0$ (the Coriolis parameter neglected). The results proved to be similar to those presented in **Table 1**. So the generated unstable disturbances are due to intense zonal wind shear.

Unstable perturbation or vortices behaviour develops in the polar regions of Venus as a response to processes of barotropic instability of a zonal flow. These results are consistent with earlier studies of barotropic instability on Venus given in Refs. [24, 34, 35] and others, who were seeking a possible origin for the Venus polar dipole features observed by Pioneer Venus.

New data of zonal wind of the middle atmosphere to cover a wide range of latitudes in the NH will help to know about the unstable perturbation that develops in the polar regions of Venus NH as a response to processes of barotropic instability. It has been shown that the Venus polar dipole is a permanent feature in the Venusian atmosphere and that it is confined to latitudes higher than 75° S [25, 33].

Simmons et al. [11] showed that barotropic instability can be responsible for a low-frequency variability of Earth's atmosphere, and Perez-Garcia [15] demonstrated that unstable perturbations are observed in the neighbourhood of subtropical jets on the Earth. Then an analytic dipole vortex may be constructed on the Venus Polar Regions. This would be called a Verkley's polar modon [17] with different dynamical configurations. Venusian atmosphere has given us not just the opportunity to learn from this initial work, but also to continue research on this topic. Our next challenge is to analyse the barotropic instability of the Zonal Flow seen in **Figure 1**, coupled with Verkley's polar modon.

3. Global monsoon system, tropical dipole vortices and tropical cyclones

NCAR-ds627.0 and NCEP/NCAR Reanalysis data were used. In particular, we used the relative humidity, the zonal (u) and meridional (v) components of the wind field at different pressure levels. These wind components are further used in the calculation of their corresponding velocity potential and stream function.

Figure 3 shows the mean of 200–250mbar stream function monthly and tropical cyclone tracks for April. A noticeable feature in **Figure 3(a)** is the basic patterns of the circulation associated with monsoon land heating at the equator in the African region monsoon, 10°–40° E, Asian-Australian monsoon, 60°–180° E and South-American monsoon, 80°–40° W. The Australian summer monsoon influences the climate of the Australian tropics during the period of December–March [37]. The onset of the Australian summer monsoon occurs in late December and typically retreats in April [38].

The early arrival of the Indian summer monsoon and North American early summer monsoon are shown in **Figure 3(b)**. The wet season of the Asian monsoon system begins in May and ends in October and the dry phase occurs in the other half of the year [39]. The set of these local monsoon systems is called the global monsoon system [40]. Liu and Zorita [41] defined the

local summer as May through September (MJJAS) in NH and November through March (NDJFM) for SH.

The American monsoon is determined by the dynamic processes of the interaction between the American continent, the eastern Pacific, the Atlantic Ocean and the overlying atmosphere [42]. The intense heat from the land creates rising of air and a surface low pressure, with low-level air flowing towards the convective regions and divergence in the upper troposphere, then the tropical cyclone moves towards the convective regions of the heated continents (**Figures 3(a)** and **4(b)**).

An important feature of the upper troposphere of a monsoon system is the high-level anticyclone (HLA) located above and to the north of the monsoon trough. The clockwise flow around this anticyclone contains an easterly jet stream in its southern flank called tropical easterly jet [43] and in the lower troposphere, for example, in North America late summer contains a maritime-continental thermal low (**Figure 5**).

In the Indian Ocean, the tropical cyclones mainly occur during pre-monsoon and post-monsoon seasons. In western North Pacific, TC most generally begins from June and ends in November [44]. Gray [45] estimates that the majority of TCs originate in or are just polewards of the Intertropical Convergence Zone [ITCZ] or monsoon trough. The upper tropospheric flow patterns over the region of storm formation control their formation and movement. Some storms recurve under the influence of a high-level anticyclone or an approaching westerly troughs of middle latitudes that extends into the upper levels of lower latitudes where east winds occur in the surface layers.

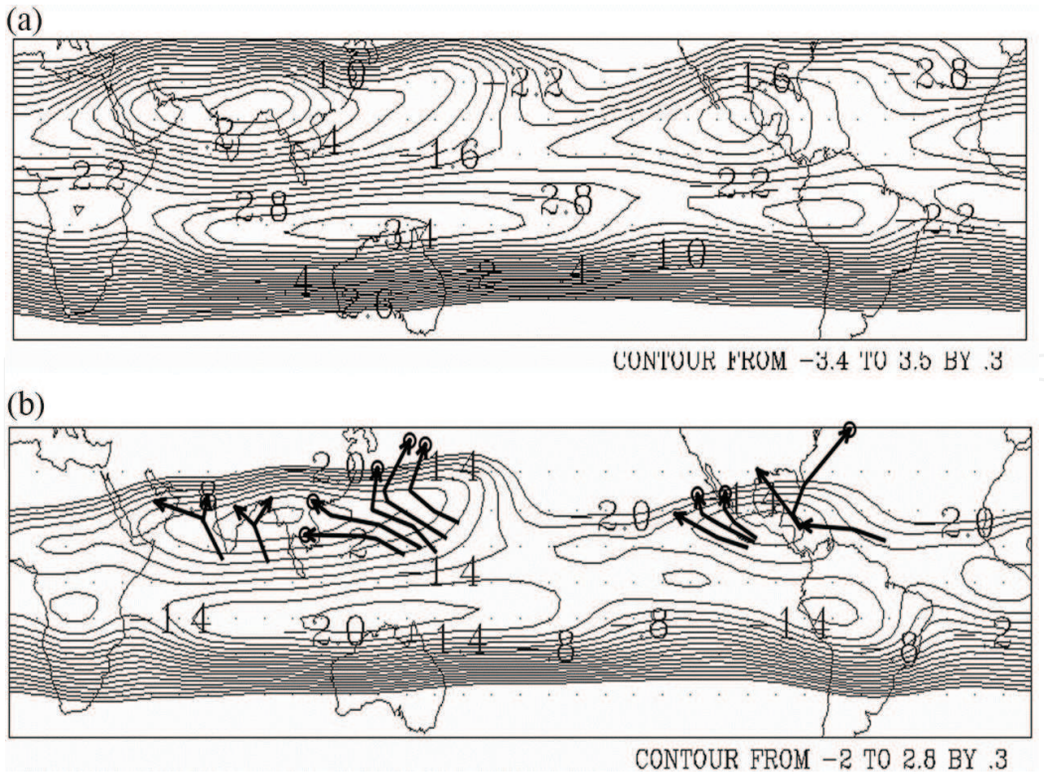

Figure 4. Isolines of the monthly stream function multiplied by 10^7 for September (a) and October (b) mean 200–250 mbar, respectively. Tropical cyclone tracks in (b) are adapted from Ref. [36].

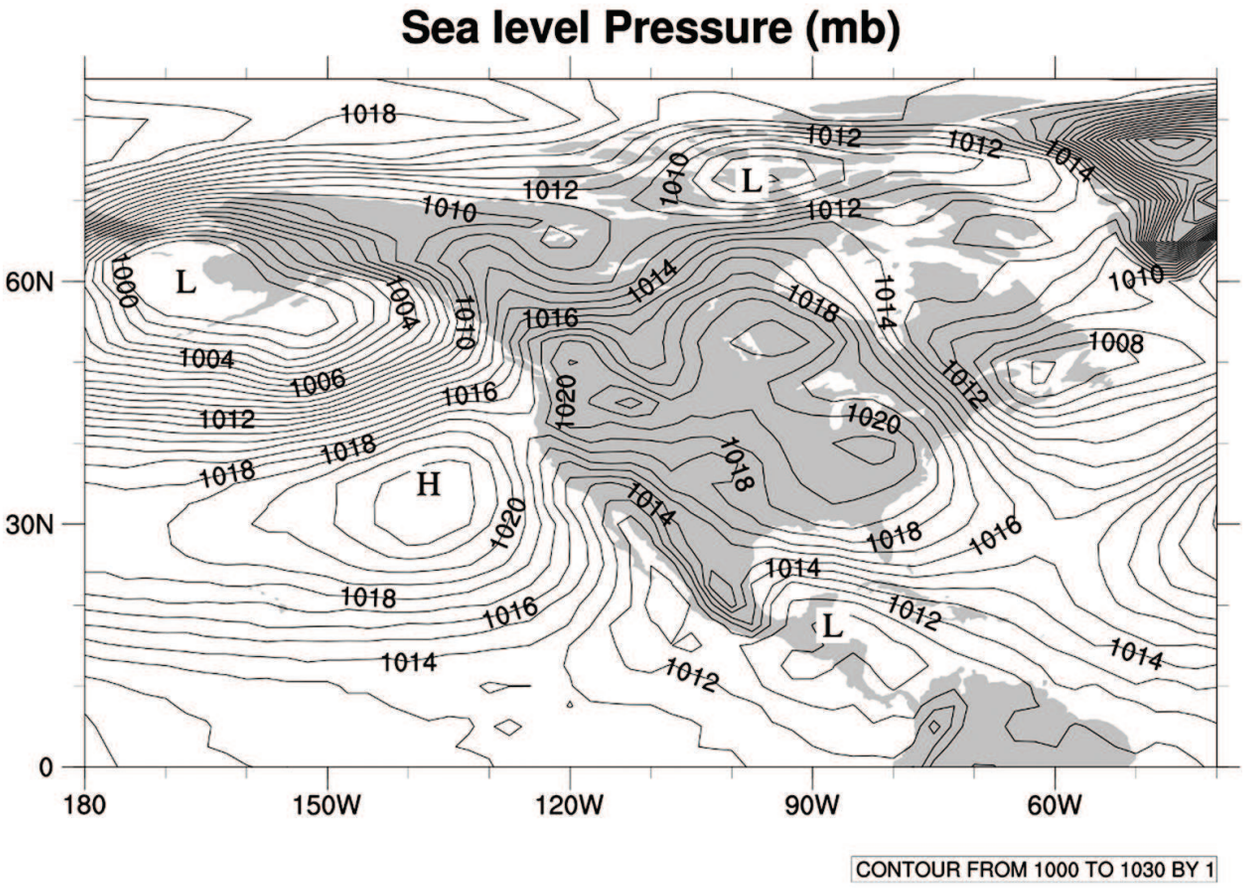

Figure 5. Sea level pressure composite, mean October 17–November 04, 1998, adapted from NOAA/ESRL.

In the Atlantic Ocean, the tropical cyclones mainly occur during May–October. In the lower troposphere, westward traveling tropical wave disturbances move in the trade wind flow across the Atlantic Ocean. They begin appearing as early as April/May and continue until October/November. Burpee [46] documented a mechanism for the origins of these waves, the instability of the African easterly jet.

An interesting feature occurs during months of May, September-November in the American monsoon system, in which its upper levels are formed with an anticyclone HLA on the northern side and an anticyclone HLC (high-level cyclone at NH) on its southern side. As a result, in certain periods, for example between September and November, the HLC and HLA remain coupled and then form a bipolar vortex or coupled monsoon system North American monsoon system (NAMS) late, and South American monsoon system (SAMS) early [6]. This bipolar vortex has a similar configuration to the Gill-Matsuno wave [47].

The genesis of Mitch was given by Refs. [6, 48–50]. In this chapter, we are interested in studying its trajectory. Why did it changed its direction south-westward during the period of October 26–28, 1998? And how the interaction with HLA and HLC may have contributed to change its path south-westward? Due to the variation of the Coriolis parameter, a cyclone embedded in a resting atmosphere moves north-westwards [51].

http://dx.doi.org/10.5772/65953

In **Figure 6(a)** and **(c)** we get a general idea that the trajectory HLA and HLC took. By October 26–27, 00Z, HLA acquired a movement almost axi–symmetric with a north-eastern flow on its southeast side. HLC was moving west-north-westward very quickly, while HLA headed north-eastward, merging together as a coupled system (Bipolar Vortex), apparently starting an anticyclonic rotation (**Figure 6(a–c)**). Because Mitch was much closer to HLA, it was guided by the HLA circulation.

On October 26th HLA was situated on the Mexican plateau along with three other anticyclone disturbances, while HLC also had three more perturbations involved with it. The tracks of HLA and HLC and their multiple disturbances by October 27 are shown in **Figure 6(b)**, merging together, demonstrating their clockwise rotation.

During October 27–28, HLA changed direction, returning south-westward; however, HLC dispersed in a westward direction. In order to examine these interaction processes, the numer-

Figure 6. Streamline mean 850–200 mbar and tracks (wide lines) of vortices HLC, HLA and tropical cyclone Mitch, the maps is for days 26 (a), 27 (b) and 28 (c) of October 1998-00Z respectively. The small circle in (b) indicates the dates 00Z (white) and 12Z (black).

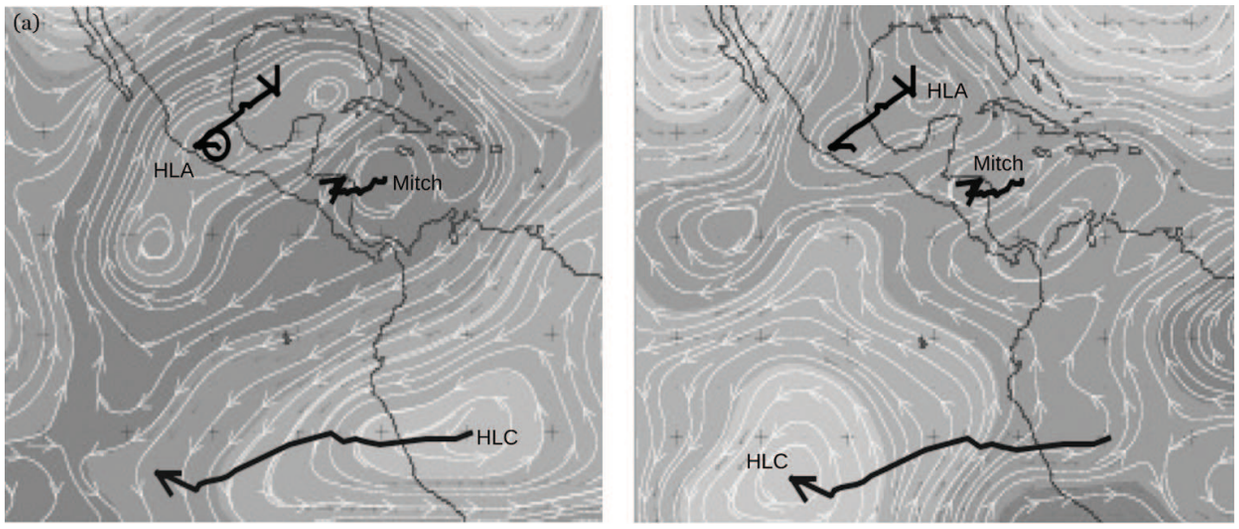

Figure 7. Streamline mean 850-200 mbar of non-divergent wind for October 26, 1998-00Z (a), and streamline mean 850–200 mbar calculated for October 28-00Z in the integration of BVE (b). Wide lines represent tracks of vortices HLC, HLA and Mitch in the period October 26–28, 1998-00Z.

ical spectral of nonlinear barotropic model (1), in truncation T31, was integrated in the time, with the initial stream-function corresponding to October 26th-00Z, 800–200 mbar mean layer (see **Figures 6(a)** and **7(a)**).

The 2-day integrations carried out with the model show that the geometric structure (comparing **Figures 6** and **7**) of the solution can be calculated to a good approximation. On October 27th, the solution HLC moved westward very fast, while HLA headed north-eastward and then became quasi-stationary. Also, HLA and HLC as a coupled system rotated in a clockwise direction as given in **Figure 6(c)**.

The formation, development and evolution of the tropical cyclone Mitch was not a process by which isolated vortices were solely involved, but rather a result of a very complicated and precise conditions, which interacted among themselves and by nearby flows. In the case described here, these nearby flows were associated with the bipolar vortex formed by late NAMS and early SAMS.

Acknowledgements

The authors are grateful to A. Salas, E. Azpra, F. Villacaña, O. Delgado, R. Patiño and L. Meza for the map analysis. We thank Nat Aguilar and an anonymous reviewer for their useful comments that helped to improve the manuscript. The data was provided by NCAR's Data Support Section (DSS). The National Science Foundation is NCAR's sponsor.

Author details

Ismael Perez-Garcia*, Alejandro Aguilar-Sierra and Jaime Hernández

*Address all correspondence to: ismael@unam.mx

Laboratory of Modeling of Atmospheric Processes, Atmospheric Science Center UNAM, (Mexican National Autonomous University), Mexico City, Mexico

References

[1] R. J. Reed, "A study of a characteristic type of upper-level frontogenesis," J. Meteorol., vol. 12, pp. 226–237, 1955.

[2] Garate-Lopez, I. R. Hueso, A. Sanchez–Lavega, and A. G. Munoz, "Potential vorticity of the south polar vortex of Venus," J. Geophys. Res., vol. 121, pp. 574–593, 2016.

[3] J. Peralta, R. Hueso, and A. Sanchez-Lavega, "Assessing the long-term variability of Venus winds at cloud level from Virtis–Venus express," Icarus, vol. 217, no. 2, pp. 585–598, 2012.

[4] C. B. Leovy, "Rotation of the upper atmosphere of Venus," J. Atmos. Sci. Vol. 30, pp. 1218-1220, 1973.

[5] S. S. Limaye, J. P. Kossin, C. Rozo, G. Piccioni, D. V. Titov, and W. J. Markiewicz, "Vortex circulation on Venus: Dynamical similarities with terrestrial hurricanes," Geophys. Res. Lett, vol. 36, L04204, 2009.

[6] I. Perez–Garcia, A. Aguilar, and J. Hernandez, "Patterns that led to the development of tropical cyclone Mitch (1988): A tribute to the affected," in preparation for publication, 2016.

[7] A. Sanchez-Lavega, "Variable winds on Venus mapped in three dimensions," Geophys. Res. Lett., vol. 35, L13204, 2008.

[8] R. Moissl, et al., "Venus cloud top winds from tracking uv features in Venus monitoring camera images," J. Geophys. Res., vol. 114, 2009.

[9] S. S. Limaye, C. G. Grasotti, and M. J. Kuetemeyer, "Venus: Cloud level circulation during 1982 as determined from pioneer clout photo-Polari meter images time and zonally averaged circulation," Icarus, vol. 73, pp. 193–211, 1988.

[10] I. Perez–Garcia and Y. N. Skiba, "Simulation of exact barotropic vorticity equation solutions using a spectral model," Atmósfera, vol. 12, pp. 223–243, 1999.

[11] A. J. Simmons, J. M. Wallace, and G. W. Branstator, "Barotropic wave propagation and instability, and atmospheric teleconnection patterns," J. Atmos. Sci., vol. 40, pp. 1363–1392, 1983.

[12] J. S. Frederiksen, "A unified three–dimensional instability theory of the onset of blocking and cyclogenesis," J. Atmos. Sci., vol. 39, pp. 969–982, 1982.

[13] G. J. Shutts, "The propagation of eddies in diffluent jet streams: Eddy vorticity forcing of 'blocking' flow fields," Quart. J. Roy. Meteor. Soc., vol. 109, pp. 737–761, 1983.

[14] H. Nakamura, M. Nakamura, and J. L. Anderson, "The role of high and low-frequency dynamics in blocking formation," Mon. Wea. Rev., vol. 125, pp. 2074–2093, 1997.

[15] I. Perez–Garcia, "Rossby–Haurwitz perturbation under tropical forcing," Atmósfera, vol. 27, pp. 239–249, 2014.

[16] P. Wu and W. T. M. Verkley, "Non–linear structures with multivalued relationships – exact solutions of the barotropic vorticity equation on a sphere," Geophys. Astro. Fluid, vol. 69, pp. 77–94, 1993.

[17] W. T. M. Verkley, "The construction of barotropic modons on a sphere," J. Atmos. Sci., vol. 41, pp. 2492–2504, 1984.

[18] W. T. M. Verkley, "Stationary barotropic modons in westerly background ows," J. Atmos. Sci., vol. 44, pp. 2383–2398, 1987.

[19] W. T. M. Verkley, "Modons with uniform absolute vorticity," J. Atmos. Sci., vol. 47, pp. 727–745, 1990.

[20] J. J. Tribbia, "Modons in spherical geometry," Geophys. Astro. Fluid, vol. 30, pp. 131–168, 1984.

[21] E. C. Neven, "Quadrupole modons on a sphere," Geophys. Astro. Fluid, vol. 65, pp. 105–126, 1992.

[22] J. Pedlosky, "Finite-amplitude baroclinic waves in a continuous model of the atmosphere," J. Atmos. Sci., vol. 36, pp. 1908–1924, 1979.

[23] R. Young and J. Pollack, "A three–dimensional model of dynamical processes in the Venus atmosphere," Atmos. Sci., vol. 34, pp. 1315–1351, 1977.

[24] L. S. Elson, "Wave instability in the polar region of Venus," J. Atmos. Sci., vol. 39, pp. 2356–2362, 1982.

[25] I. Garate–Lopez, R. Hueso, A. Sanchez–Lavega, J. Peralta, G. Piccioni, and P. Drossart, "A chaotic long-lived vortex at the southern pole of Venus," Nat. Geosci., vol. 6, pp. 254–257, 2013.

[26] Y. N. Skiba and I. Perez–Garcia, "Numerical spectral method for normal–mode stability study of ideal ows on a rotating sphere," Int. Jour. Appl. Mat., vol. 22, pp. 725–758, 2009.

[27] I. Perez–Garcia and Y. N. Skiba, "Tests of a numerical algorithm for the linear instability study of ows on a sphere," Atmosfera, vol. 14, pp. 95–112, 2001.

[28] L. Rayleigh, "On the stability of certain fluid motions," Proc. London Math. Soc., vol. 11, pp. 57–70, 1880.

[29] H. L. Kuo, "Dynamic instability of two-dimensional non-divergent flow in a barotropic atmosphere," J. Meteor., vol. 6, pp. 105–122, 1949.

[30] F. Baer, "Studies in low-order spectral systems," Tech. rep., Colorado State University, Department of Atmospheric Physics, 1968.

[31] Y. N. Skiba, "On the normal mode instability of harmonic waves on a sphere," Geophys. Astro. Fluid, vol. 92, pp. 115–127, 2000.

[32] R. Fjortoft, "On the changes in the spectral distribution of kinetic energy for two-dimensional non-divergent ow," Tellus, vol. 5, pp. 225–230, 1953.

[33] G. Piccioni, "The many faces of the Venus polar vortex," European Planetary Science Congress, vol. 5, pp. 2010–2480, 2010.

[34] D. V. Michelangeli, R. Zurek, and L. S. Elson, "Barotropic instability of midlatitude zonal jets on Mars, Earth and Venus," J. Atmos. Sci., vol. 44, pp. 2031–2041, 1987.

[35] A. R. Dobrovolskis and D. J. Diner, "Barotropic instability with divergence: Theory and applications to Venus," J. Atmos. Sci., vol. 47, no. 3, pp. 1578–1588, 1990.

[36] H. L. Crutcher and R. G. Quayle, "Mariners worldwide climatic guide to tropical storms at sea," Tech. rep., US Navy, 1974.

[37] Carvalho, Leila Maria Véspoli de; Jones, Charles, The Monsoons and Climate Change: Observations and Modeling, Springer climate, ISBN 978-3-319-21650-8, 2016.

[38] C. W. Hung and M. Yanai, "Factors contributing to the onset of the Australian summer monsoon," Quart. J. Roy. Meteor. Soc., vol. 130, pp. 739–758, 2004.

[39] P. J. Webster, T. Palmer, M. Yanai, R. Tomas, V. Magaña, J. Shukla, and A. Yasunari, "Monsoons: Processes, predictability and the prospects for prediction," J. Geophys. Res. (TOGA special issue), vol. 7, p. 14, 1998.

[40] C. P. Chan, B. Wang, and G. Lau. (Eds.). The Global Monsoon System: Research and Forecast. Report of the International Committee of the Third 22 International Workshop on Monsoons (IWM-III). WMO/TD, No. 1266. Tropical Meteorology Research Programme (TMRP). Report No. 70. November 2004.

[41] J. Liu and E. Zorita, "Centennial variations of the global monsoon precipitation in the last millennium: results from echo–g model," J. Climate, vol. 22, pp. 2356–2371, 2009.

[42] A. Chakraborty and T. N. Krishnamurti, "Numerical simulation of the North American monsoon system," Meteorol Atmos Phys, vol. 84, pp. 57–82, 2003.

[43] B. Hoskins and B. Wang, The Asian Monsoon, Ch. Large-Scale Atmospheric Dynamics, Springer, Berlin Heidelberg, pp. 357–415, 2006.

[44] L. Chen and Y. Ding, An Introduction to the Typhoon Over Western Pacific. Science Press, Beijing, 1979.

[45] W. M. Gray, "Global view of the origin of tropical disturbances and storms," Mon. Wea. Rev., vol. 96, pp. 669–700, 1968.

[46] R. W. Burpee, "The origin and structure of easterly waves in the lower troposphere of North Africa," J. Atmos. Sci., vol. 29, pp. 77–90, 1972.

[47] A. E. Gill, "Some simple solutions for heat induced tropical motion," Quart. J. Roy. Meteor. Soc., vol. 449, pp. 447–462, 1980.

[48] J. L. Guiney and M. B. Lawrence, "Hurricane Mitch 22 October–05 November 1998," Tech. rep., National Hurricane Center, NOAA, 1999.

[49] L. A. Avila, R. J. Pasch, and J. L. Guiney, "Atlantic hurricane season of 1998," Mon. Wea. Rev., vol. 129, pp. 3085–3123, 2001.

[50] Hernández, J. (2016). Interaction of North American summer anticyclone and tropical cyclones: study of specific cases. (M. Sc. thesis), Autonomous National University of Mexico, Mexico City.

[51] J. Adem, "A series solution for the barotropic vorticity equation and its application in the study of atmospheric vortices," Tellus, vol. 8 (3), pp. 364–372, 1956.

IntechOpen